Hindawi
Advances in Materials Science and Engineering
Volume 2019, Article ID 7523492, 9 pages
https://doi.org/10.1155/2019/7523492

Research Article

Preparation of a Cenosphere Curing Agent and Its Application to Foam Concrete

Zhongwei Liu,[1,2] **Kang Zhao**,[1] **Yufei Tang**,[1] **and Chi Hu**[2]

[1]*Department of Materials Science and Engineering, Xi'an University of Technology, Xi'an 710048, China*
[2]*Sichuan College of Architectural Technology, Deyang 618000, China*

Correspondence should be addressed to Kang Zhao; kzhao@xaut.edu.cn

Received 24 October 2018; Accepted 16 January 2019; Published 3 March 2019

Academic Editor: Andres Sotelo

Cenospheres are hollow and spherical particles extracted from fly ash. Controllable separation of cenosphere particles with different densities and sizes can be realized by controlling the density of a flotation solution of cenospheres. In this paper, cenospheres were corroded by hydrofluoric acid to produce perforated pores on their shell surfaces. Then, the cenospheres were mixed with water to prepare the cenosphere curing agent. Foam concrete was prepared using ordinary Portland cement (42.5 R), vegetable protein foaming agent, fly ash, cenospheres, and the cenosphere curing agent as raw materials. The water absorption rate of the cenosphere curing agent was 156.0 wt.%, and 85% of the loaded water was released at a relative humidity of 97.4%, which met the microenvironment requirements of foam concrete. Addition of the cenosphere curing agent during foam concrete preparation has the following positive functions for foam concrete: inhibiting autogenous shrinkage, promoting the hydration degree, improving the state of the interfacial transition zone between cenospheres and the hardened cement paste, reducing the number of connected pores, relieving the stress concentration on the pore walls, and enhancing the compression strength of the foam concrete.

1. Introduction

Foam concrete includes no aggregates but contains a large number of cementitious materials. Thus, the autogenous shrinkage of foam concrete is greater than that of ordinary concrete, which leads to cracking and reduces the durability of foam concrete. Because of these defects, the applications of foam concrete in the field of building insulation are limited. Some scholars believe that internal curing of foam concrete can reduce its autogenous shrinkage safely and effectively [1, 2].

The key step in internal curing is selection of the appropriate internal curing agent which is used to load and release water. An ideal internal curing agent should be able to release most of its loaded water evenly at a high relative humidity. At present, super absorbent polymer [3–7] and inorganic porous aggregates [8–14] are employed as two types of internal curing materials. However, super absorbent polymer exerts adverse effects on the rheological property, mechanical properties, and impermeability of the final concrete, while porous aggregate causes deterioration of its elastic modulus and compressive strength [15–17]. Cenospheres are excellent potential industrial waste byproduct because of many benefits, such as low density, excellent mechanical strength, and reasonable cost when used as a light weight aggregate or as an additive in concrete production [18, 19]. Barbare et al. [20] found that cenospheres released moisture at a constant speed over a certain period of time during drying. Liu et al. [21, 22] prepared perforated cenospheres by acid etching of the glass-crystalline nanosized film on the surface of the cenosphere shells and then filled these spheres with water; the water-loaded spheres were subsequently used as the internal curing agent for concrete. This approach overcomes the obvious disadvantages of a super absorbent polymer and inorganic porous aggregates. Bentz and Snyder [23] found that cement paste should lie within a sufficiently small distance from the internal curing water reservoir so that the internal water could

penetrate. To achieve this, the internal curing agent particle size should be as small as possible. However, further reduction of the internal curing agent particles led to the reduction of internal curing efficiency. Zhutovsky et al. [24] found that this apparent discrepancy was caused by two competing mechanisms taking place upon reduction of the particle size of the internal curing agent: (1) small spacing factor can enhance the internal curing efficiency, and (2) small particles have smaller pores which tend to hold water more tightly, making them unavailable for internal curing, leading to reduction of internal curing efficiency. Wei et al. [25] confirmed that the internal curing effect was the greatest when the ratio of the distance between the internal curing agents and their particle size was 1.1. Therefore, the particle size of internal curing agents cannot be excessively large, and the curing agent with very large particle sizes cannot be embedded into the thin pore wall of the foam concrete.

In this paper, controllable separation of cenospheres with different densities and particle sizes was achieved by tuning the concentration of the flotation solution. Then, an internal curing agent suitable for foam concrete production was prepared by corrosion of the cenospheres and mixed with 800 kg/m^3 foam concrete. The matrix compactness, internal humidity, autogenous shrinkage, and physical and mechanical properties of the foam concrete were then evaluated.

2. Materials and Methods

2.1. Raw Materials. Ordinary Portland cement (42.5 R) was purchased from Sichuan Deyang Lisen Cement Co., Ltd. and I-level fly ash was from Jiangyou Thermal Power Plant. Tables 1 and 2 show the physical properties and chemical composition of cement and fly ash, respectively. Cenospheres were purchased from Henan Borun Co., Ltd., and Table 3 shows their chemical composition. Plant protein foaming agent (Sichuan Xinghan Anticorrosion and Insulation Engineering Co., Ltd.), hydrochloric acid, and ammonium fluoride were used in the experiments. All of these reagents were of analytical purity.

2.2. Preparation of the Cenosphere Curing Agent. Cenosphere curing agent was prepared through (1) flotation and (2) corrosion.

2.2.1. Flotation of Cenospheres. The flotation device is shown in Figure 1. The flotation process of cenospheres was carried out according to the following steps: (1) Absolute ethanol was mixed with water as the flotation solution to achieve a certain concentration of the alcoholic solution. (2) The original cenospheres (without flotation; marked F0) were poured into the flotation device and completely mixed with 55 wt.% anhydrous ethanol solution. (3) The mixture was allowed to stand for 2 min, after which the cenospheres at the bottom were quickly discharged from the bottom of the device. The remaining cenospheres in the flotation device were poured onto a tray and dried in an oven to obtain the primary cenospheres sample (marked F1). (4) The primary cenospheres sample was mixed with 85 wt.% anhydrous ethanol solution. (5) The mixture was allowed to stand for 2 min, after which the cenospheres at the bottom were quickly discharged from the bottom of the device. The cenospheres discharged from the bottom were poured onto the tray and dried in the oven to achieve the secondary cenospheres sample (marked F2).

Table 1: The physical properties of cement and fly ash.

Cement		Fly ash	
Blaine fineness (m^2/kg)	343	Particle size (45 μm sieve rate) (%)	2.9
Initial setting time (min)	91	Ratio of water demand (%)	91.0
Final setting time (min)	210	Water content (%)	0.2
Soundness	Qualified	Activity index (%)	66.0
3 d compressive strength (MPa)	28.7	Density (g/cm^3)	2.6
28 d compressive strength (MPa)	48.9	–	–

2.2.2. Corrosion of Cenospheres. To introduce water into the cavity of the cenospheres, perforated cenospheres were prepared by corroding the glass-phase film on the shell surfaces of the cenospheres and filling them with water [26]. Then, 100 mL hydrofluoric acid corrosion solution with a concentration of 0.6 mol·L^{-1} was prepared using NH_4F and hydrochloric acid. Approximately 40 g of cenospheres were immersed in the hydrofluoric acid corrosion solution and stirred magnetically for 9 min at 120 r/min. After corroded cenospheres were filtered and washed thoroughly with plenty of water, they were dried in an oven at 110°C, and perforated cenospheres were obtained. It must be pointed out that the waste solution containing hydrofluoric acid is hazardous. It can be easily removed by adding the solution of calcium hydroxide. The perforated cenosphere samples achieved by corroding F0 and F2 sample were labeled E0 and E2, respectively.

2.3. Preparation of Foam Concrete. In accordance with ASTM C128-15 [27], the E2 sample was prepared into saturated surface dry perforated cenospheres (internal curing agent). The internal curing agent was mixed with foam concrete to evaluate the effect of the internal curing agent on the internal humidity, autogenous shrinkage, and compressive strength of the foam concrete. The foam concrete was prepared through the following steps: (1) Cement, fly ash, F2, E2 (internal curing agent), and water were added to a mixer (GH-15, Beijing Guanghui Jingyan Foam Concrete Technology Co., Ltd.) in accordance with the mixing ratio in Table 4. The mixture was combined for 2 min at 40 r/min to prepare a cement slurry. (2) The foaming agent and water were combined at a ratio of 1 : 15 and foamed using a foaming machine (ZK-FP-20, Beijing Zhongke Zhucheng Building Materials Technology Co., Ltd.). (3) The foam was added to the cement slurry in accordance with the mixing ratio in Table 4 and stirred at 40 r/min to combine

Table 2: The main chemical composition of cement and fly ash (wt.%).

Composition	SiO_2	Al_2O_3	Fe_2O_3	CaO	MgO	SO_3	Na_2O	K_2O	TiO_2	Loss of ignition
Cement	21.6	4.9	2.50	63.4	1.80	2.14	0.14	0.37	–	3.15
Fly ash	57.80	24.84	4.60	4.74	2.45	2.60	1.20	–	0.50	0.90

Table 3: The main chemical composition of cenospheres before and after chemical corrosion (wt.%).

Composition	SiO_2	Al_2O_3	CaO	Fe_2O_3	TiO_2	MgO	Na_2O	K_2O	P_2O_5
Original cenospheres	58.35	31.43	0.43	2.26	1.18	0.53	0.55	1.41	0.05
Perforated cenospheres	58.81	34.50	0.32	2.12	1.16	0.50	0.53	1.32	0.05

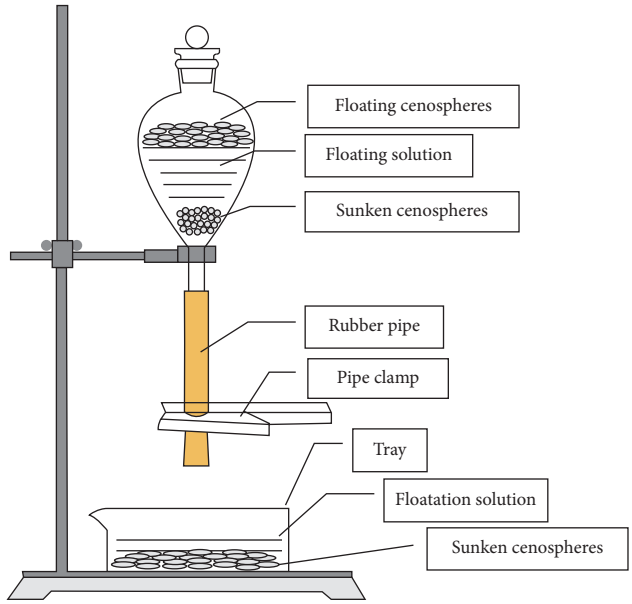

Figure 1: Schematic drawing of flotation device.

Table 4: Mix proportions of foam concrete.

Mixes designation	Design density (kg/m^3)	Cement (g)	Fly ash (g)	Foam (mL)	Water-binder ratio	F2 (g)	E2 (g)	Net water (g)	Water absorbed in cenospheres (g)
800-C	800	4723	1181	2868	0.50	0	0	2952	0
800-F2	800	4723	1181	2868	0.50	117	0	2952	0
800-E2	800	4723	1181	2868	0.50	0	117	2952	271

the foam with the cement slurry thoroughly. (5) Finally, the mixture was cast, molded, and subjected to standard curing for 28 d (temperature: $20 \pm 2^{\circ}C$; relative humidity: >95%).

3. Results and Analysis

3.1. Flotation of Cenospheres. The morphologies of F0 and F2 were characterized by scanning electron microscopy (SEM; SU-3500; Hitachi High-technologies Corporation). The images were binarized, and the results are shown in Figure 2. The particle sizes of each cenosphere in the images were measured by Image-Pro Plus 6.0 software, and the particle size distribution of the cenospheres was calculated (Figure 3).

As shown in Figure 2, after two cycles of flotation, the broken cenospheres were effectively removed from the original cenospheres. In Figure 3, the proportion of cenospheres with particle sizes between 20 and 40 μm was 75.0% in the F2 sample after flotation but only 55.2% in the F0 sample (original cenospheres). Thus, the flotation of cenospheres with the flotation solution as the medium effectively decreased cenospheres with particle sizes less than 20 μm and removed those with particle sizes greater than 50 μm. This step narrowed the particle size distribution of the cenospheres.

3.2. Corrosion of Cenospheres. Table 3 lists the main chemical composition of the cenospheres before and after corrosion. The content of alumina in the cenospheres increased from 31.43% to 34.50% because some metal oxides in the cenosphere shell, such as CaO, Fe_2O_3, Ti_2O, and MgO, were easily

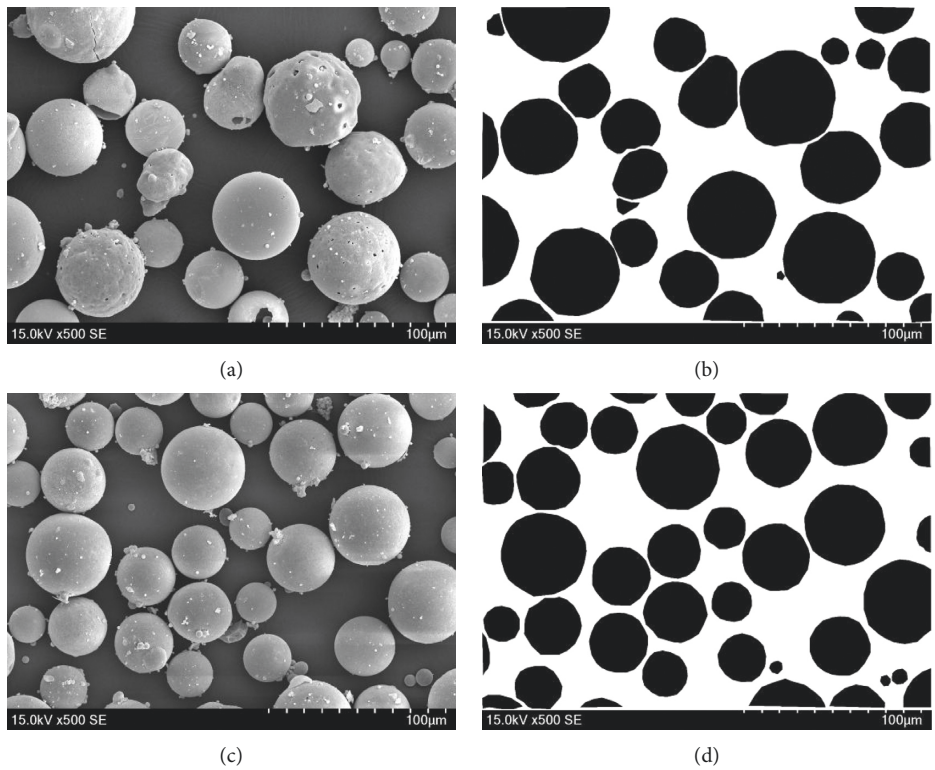

Figure 2: SEM microphotographs of the cenospheres before and after flotation. (a) Original image of F0. (b) Binarization processing image of F0. (c) Original image of F2. (d) Binarization processing image of F2.

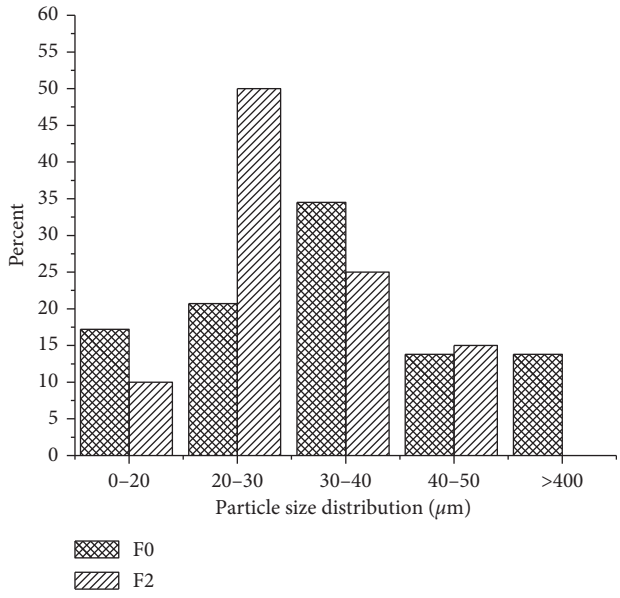

Figure 3: The particle size distribution of the cenospheres before and after flotation.

corroded and dissolved by hydrofluoric acid. However, Al_2O_3 and SiO_2 are difficult to corrode and dissolve by hydrofluoric acid [21, 22]. Thus, their relative contents increased, resulting in 8.69% quality loss of the cenosphere shells. Figure 4(a) displays an SEM image of the cenospheres before corrosion. The shell of the cenospheres was highly dense before corrosion, and water could not enter the spheres. Figure 4(b) displays an SEM image of the cenospheres after corrosion by hydrofluoric acid. Perforated holes were formed on the shell of the spheres, which allowed water to enter or be released from their cavities.

3.3. Water Absorption and Releasing Performance of the Cenosphere Curing Agent. In accordance with ASTM C128-15 [27], the water absorption properties of the cenosphere curing agent can be determined by measuring the difference between the absolute dry weight and the saturated surface dry weight of the cenospheres. The water absorption of sample E0 and E2 was 118 wt.% and 153 wt.%, respectively. The water absorption rate of the perforated cenospheres was substantially increased by flotation, which enabled the effective removal of broken cenospheres and reduction of those spheres with particle sizes less than 20 μm or a small cavity volume.

The water release characteristics of saturated perforated cenospheres are crucial to the internal curing effect [20, 21]. The perforated cenospheres were mixed with water until all of the spheres sank to the bottom of the container. Then, the cenospheres at the bottom of the container were collected, filtered, and finally prepared into saturated surface dry cenospheres (internal curing agent) in accordance with ASTM C128-15 [27]. Deionized water was used to prepare environment with relative humidity of 100%. Saturated K_2SO_4, KNO_3, KCl, and NaCl salt solutions were used to prepare environments with relative humidities of 97.4%, 94.2%, 85.5%, and 75.6% in accordance with ASTM E104

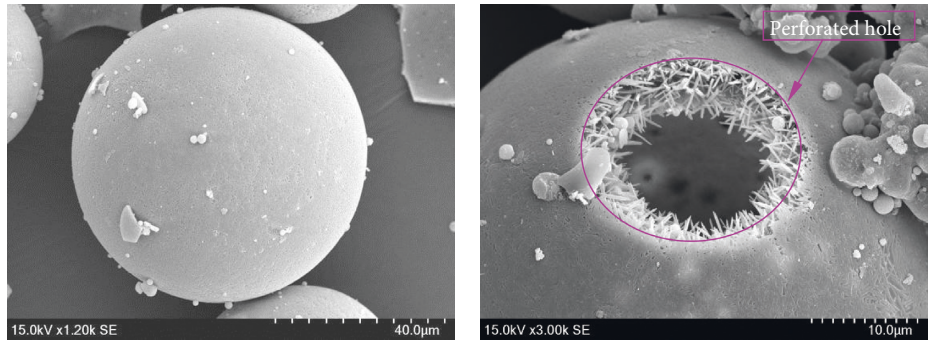

(a) (b)

Figure 4: SEM microphotograph of the cenospheres before and after corrosion. (a) The cenospheres before corrosion. (b) The perforated cenospheres after corrosion.

[28], respectively. These relative humidities are within the range of relative humidity reduction in concrete caused by self-desiccation (100%–75%) [29]. The water release characteristics of the saturated perforated cenospheres were tested by the following method. Perforated cenospheres in the saturated surface dry condition were weighed and then placed in the environment with a relative humidity of 97.4%. The perforated cenospheres were then weighed once more upon achieving a constant mass and then transferred to the next environment until a constant mass was achieved. The mass changes of perforated cenospheres in different humidity environments were calculated to obtain a water release characteristic curve.

The water release behavior of the E2 curing agent under different relative humidity environments was tested, and the results are shown in Figure 5. Most of the water carried by the saturated perforated cenospheres could be released quickly even in a high humidity environment. When the relative humidity of the environment was 97.4%, 85% of the water in the cenospheres was released. When the relative humidity was 94.2%, 98% of the water in the cenospheres was released. When the relative humidity was 85.5%, the water in the cenospheres was completely released. Research shows that the phenomenon of autogenous shrinkage occurs only when the internal relative humidity of the cement slurry drops to 96% [25]. This result indicates that the cenosphere curing agent can thoroughly meet the microenvironment requirement of foam concrete and release a large number of water prior to autogenous shrinkage. This effect is mainly achieved by the cavity structure of cenospheres with a large number of perforated holes distributed on the surface of their spherical shells. Such a simple structure can force the water to be released to the surrounding environment driven by the humidity gradient.

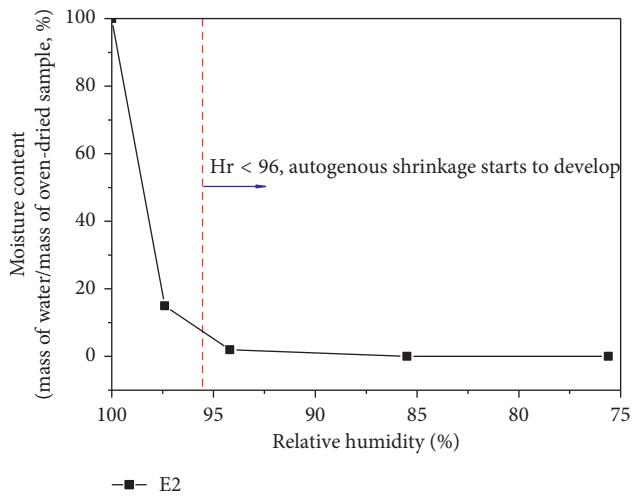

Figure 5: Water desorption properties of saturated perforated cenospheres.

3.4. Autogenous Shrinkage and Internal Humidity of the Foam Concretes. The development of autogenous shrinkage and internal humidity of foam concrete with age were measured by the integrated test method [30, 31] that simultaneously measured the shrinkage deformation and internal humidity of the samples. The dimensions of rectangular concrete specimens used for autogenous shrinkage determination were 1000 mm × 100 mm × 38 mm. One end of the specimen was fixed to the test mold, and the other end was freely expanded in the horizontal direction and connected to a linear variable differential transformer with an accuracy of 0.1 μm. The test tank was covered with 2 mm thick plastic foam to reduce the friction between the mold and the foam concrete specimen. During the autogenous shrinkage test, the specimen was completely wrapped with plastic film to block moisture exchange with the environment. Shrinkage deformation was measured when the foam concrete was completely set. A humidity sensor embedded inside the center of the foam concrete (with an accuracy of 2.0%) was used to measure the relative humidity inside the specimen.

Figure 6 presents the development curve of the internal relative humidity and autogenous shrinkage of 800 kg/m^3 foam concrete with age. A substantial difference in the development of internal humidity was noted between ordinary foam concrete samples, such as 800-C and 800-F2, and the internal curing agent-containing foam concrete sample 800-E2. At the same age, the internal humidity of the internal curing foam concrete was generally higher than that of ordinary foam concrete. The ordinary foam concrete showed an internal humidity that dropped rapidly to less than

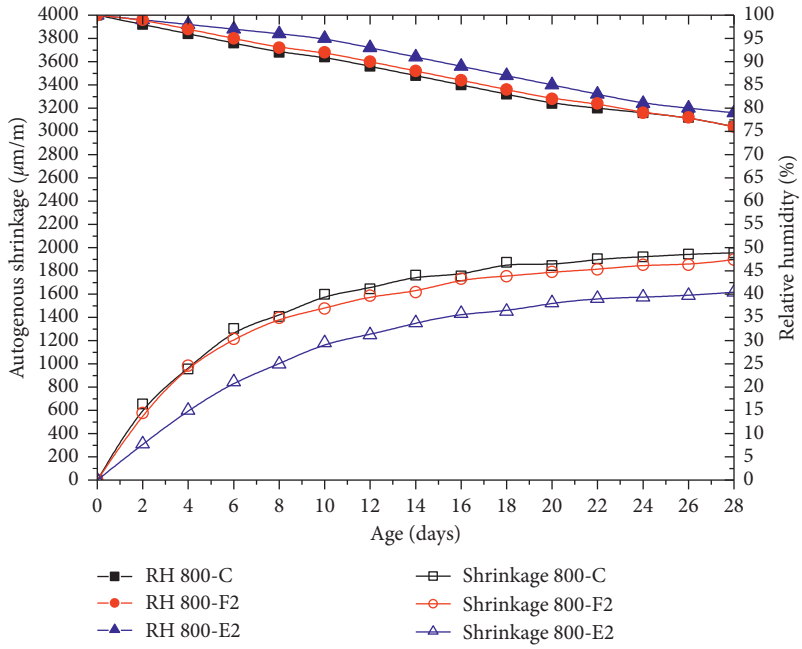

Figure 6: Interior humidity and autogenous shrinkage versus time diagrams of the foam concrete.

96% within 6 d, but the internal humidity of the internal curing foam concrete was maintained at over 96% after 8 d, gradually decreasing thereafter. The autogenous shrinkage value of sample 800-C, 800-F2, and 800-E2 at 28 d was 1954.2, 1895.7, and 1615.7 μm/m, respectively. The autogenous shrinkage of sample 800-F2 was reduced by 17.3% relative to that of specimen 800-C, likely because of the good volume stability of the cenospheres, which act as aggregates and limit the shrinkage of the foam concrete. The autogenous shrinkage of specimen 800-E2 was reduced by 19.9% relative to that of specimen 800-C. This result is attributed to several reasons: (1) the curing agent has good volume stability and can act as an aggregate to limit the shrinkage of the matrix and (2) the curing agent is dispersed evenly inside the foam concrete and forms tiny "reservoirs" that serve as a "carrier" and "Sustained-Release Capsule." The reservoir releases moisture to balance the declining relative humidity in the foam concrete system. The curing agent can effectively restrain the autogenous shrinkage of the foam concrete. Because the curing agent can maintain the internal relative humidity of the foam concrete above 96% for a considerable length of time since the beginning of pouring, the cement slurry with an internal relative humidity above 96% will not undergo autogenous shrinkage. Thus, autogenous shrinkage can be reduced.

3.5. Degrees of Hydration of the Foam Concretes. The degree of hydration of the hardened cement paste can be calculated by measuring the amount of chemically bound water [32–34] because the ratio of the amount of chemically bound water to the degree of hydration is 0.25 [35]. The amount of chemically bound water was determined by the following method. Samples that had been cured for 1, 3, 7, or 28 d were soaked in absolute ethanol to stop hydration. The samples were then finely ground and dried to a constant weight at 105°C to remove all of the evaporable water. Afterward, 2 g of the hardened cement paste sample was weighed, placed in a crucible, and then heated at 1050°C to a constant weight to remove all of the chemically bound water. The mass loss between 105°C and 1050°C was considered to be derived from the chemically bound water. The masses of the cenospheres and cenosphere curing agent were eliminated in the calculation. The chemically bound water of the cementitious material per unit mass was calculated in accordance with the following formula:

$$W_{ne} = \frac{W_1 - W_2}{W_2} - \frac{R_{fc}}{1 - R_{fc}},$$
$$R_{fc} = P_f R_f + P_c R_c, \quad (1)$$

where W_{ne} is the amount of chemically bound water (%) in cementitious material per unit mass; W_1 is the mass of the sample after being dried at 105°C (g); W_2 is the mass of the sample after ignition at 1050°C (g); R_f and R_c are the losses on ignition of the fly ash and cement, respectively (%); P_f and P_c are the mass fractions of the fly ash and cement, respectively, in the composite cementitious material (%); and R_{fc} is the loss on ignition of the raw materials in the hardened paste of the composite cementitious material per unit mass (%).

Figure 7 presents the development curve of the hydration degree of 800 kg/m^3 foam concrete with age. The degrees of hydration of 800-F2 were 0.2%, 0.2%, 1.2%, and 0.6% higher than those of 800-C at 1, 3, 7, and 28 d, respectively. This small difference in hydration degree is due to the slight variation in internal humidity between samples. The degrees of hydration of 800-E2 were 2.4%, 2.6%, 7.2%, and 9.3% higher than those of 800-C at 1, 3, 7, and 28 d, respectively; here, the difference in the degrees of hydration between 1 and 3 d was small, likely because the difference in internal humidity between 800-E2 and 800-C was less than 1% in the first 3 d of curing. However, the degree of

hydration reaction varied markedly on 7 and 28 d, possibly because the difference in internal humidity exceeded 3% between these days.

3.6. Compression Strength of the Foam Concretes. The compression strengths of 800 kg/m^3 foam concretes at 1, 3, 7, and 28 d were determined in accordance with the method specified in JG/T266-2011 for foam concretes. The test results are shown in Figure 8.

The compression strengths of 800-C at 1, 3, 7, and 28 d were 1.26, 6.39, 7.96, and 8.89 MPa, respectively. The compression strengths of 800-F2 increased by 4.8%, 2.7%, 2.3%, and 2.9% at 1, 3, 7, and 28 d, respectively, relative to those of 800-C. This result was achieved because cenospheres play a strengthening role in the action of mixing and pouring of foam concrete with good volume stability and high rigidity and strength. The compression strengths of 800-E2 increased by 7.9%, 5.2%, 10.6%, and 6.6% at 1, 3, 7, and 28 d, respectively, relative to those of 800-C. This effect was achieved because the internal curing water loaded by the saturated perforated cenospheres was released into the surrounding cement slurry and compensated for the loss of water derived from cement hydration. The curing water improved the hydration degree of the cement and ultimately improved the compression strength of the concrete.

Figure 9 shows SEM images of the microstructures of the 800-F2 and 800-E2 foam concrete samples. The cenospheres in sample 800-F2 were well preserved in the matrix, but the interface between the cenospheres and the cementitious material was very obvious. The perforated cenospheres in sample 800-E2 were not only well preserved in the matrix but also closely combined with the hydrated cementitious material, and the interface was not obvious. This result can be explained in several ways. (1) First, the cenosphere curing agent functions as a reservoir. When the relative humidity in the cement paste is reduced, the moisture in the cenosphere curing agent migrates to the cement paste. The continuous supply of moisture automatically maintains the hydration of the cement for a period of time and provides moisture for the unhydrated cement particles. This moisture retards the decrease in relative humidity of the foam concrete and promotes the hydration of the cement. The results of the hydration degree in Figure 8 also illustrate that the hydration in the internal curing foam concrete is sufficient. (2) Second, the perforated cenospheres are produced through hydrofluoric acid corrosion. The rough and porous surfaces of these cenospheres increase the mechanical meshing effect on the hardened cement paste, improve the state of the interfacial transition zone between the cenospheres and the hardened cement paste, and enhance the compression strength of the foam concrete.

Figure 10 displays SEM images of the foam concrete samples 800-C, 800-F2, and 800-E2 at 28 d. Sample 800-C reveals the largest number of connected pores, followed by 800-F2 and 800-E2. The filling effect of the perforated cenospheres can reduce the hydration reaction of the cement, delay the bursting of foam in the foam concrete mixture, and reduce the number of connected pores in the foam concrete. Foam concretes were prepared through a

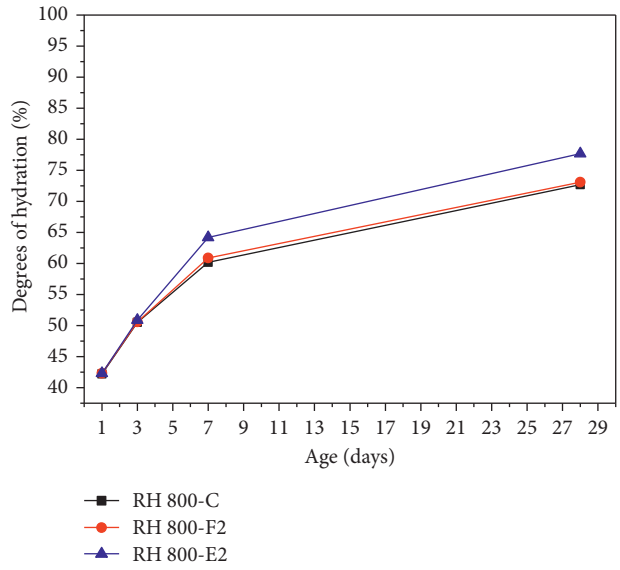

Figure 7: Degrees of hydration of the foam concrete.

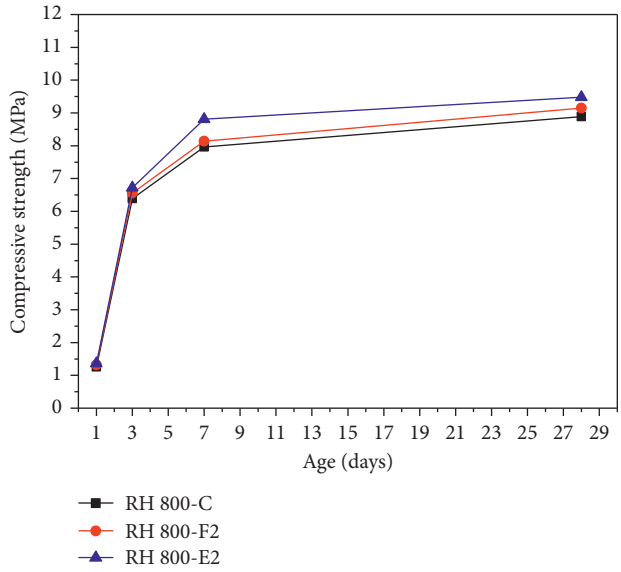

Figure 8: Compressive strengths of the foam concrete versus time.

prefoaming method in this paper; when the cement paste was mixed well with foams, the cement paste system was in a stable state [36]. Aggregating the liquid film around bubbles is the key to control physical foaming mechanisms during the manufacturing process of foam concretes [37]. The release of curing water in the cavity of the perforated cenospheres can effectively delay the bursting of bubbles in the foam concrete mixture. As a result, the number of connected pores in the foam concrete was reduced remarkably to relieve the stress concentration of the pore wall of the foam concrete and enhance its compression strength.

4. Conclusions

(1) Controllable separation of cenospheres particles with different densities and sizes could be achieved

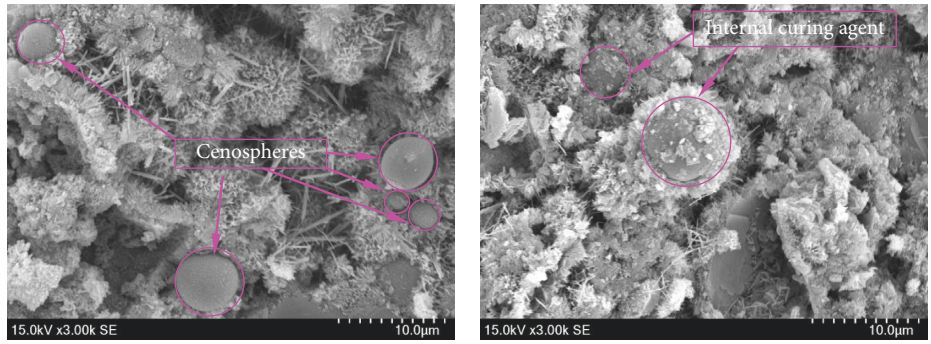

(a) (b)

Figure 9: SEM images of the microstructure of foam concrete. (a) Original image of 800-F2. (b) Binarization processing image of 800-E2.

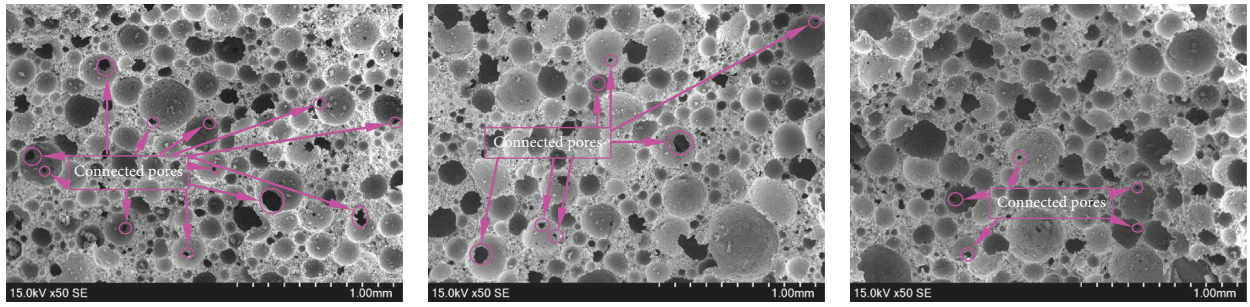

(a) (b) (c)

Figure 10: SEM images of the foam concrete. (a) SEM image of 800-C. (b) SEM image of 800-F2. (c) SEM image of 800-E2.

by controlling the concentration of the flotation solution. The proportion of sample F2 with particle sizes between 20 and 40 μm prepared in the experiment was as high as 75.0%, and the water absorption rate of the cenosphere curing agent was 156.0 wt%.

(2) Approximately 85%, 98%, and 100% of the moisture were released from the E2 curing agent under relative humidities of 97.4%, 94.2%, and 85.5%, respectively. The cenosphere curing agent could sufficiently meet the microenvironment requirements of the foam concrete.

(3) The autogenous shrinkage of sample 800-E2 at 28 d was 1615.7 μm/m, which is a reduction of 17.3% relative to that of 800-C. The hydration degree of 800-E2 at 28 d was 9.3% higher than that of 800-C, and the compression strength of the former was 6.6% higher than that of the latter at the same curing age. The internal curing effect of the cenosphere curing agent effectively delayed the reduction of internal humidity in the foam concrete, inhibited its autogenous shrinkage, increased the hydration degree of the matrix, improved the state of the interfacial transition zone between the cenospheres and the hardened cement paste, reduced the number of connected pores in the foam concrete, relieved the stress concentration on the pore wall of the foam concrete, and increased the strength of the foam concrete.

Data Availability

All data used to support the findings of this study are included within the article. and its supplementary information files used to support the findings of this study are available from the corresponding author upon request.

Conflicts of Interest

The authors declare that they have no conflicts of interest.

Acknowledgments

This work was supported by the National Natural Science Foundation of China under Grant no. 51372199.

References

[1] S.-H. Kang, S.-G. Hong, and J. Moon, "Shrinkage characteristics of heat-treated ultra-high performance concrete and its mitigation using superabsorbent polymer based internal curing method," *Cement and Concrete Composites*, vol. 89, pp. 130–138, 2018.

[2] D. Shen, X. Wang, D. Cheng, J. Zhang, and G. Jiang, "Effect of internal curing with super absorbent polymers on autogenous shrinkage of concrete at early age," *Construction and Building Materials*, vol. 106, pp. 512–522, 2016.

[3] B. Chen, J. Ding, Y. Cai, Y. Bai, and W. Zhang, "Influence of internal curing and expansive agent on concrete complex

crack resistance," *Journal of the Chinese Ceramic Society*, vol. 44, no. 2, pp. 189–195, 2016.

[4] J. Justs, M. Wyrzykowski, D. Bajare, and P. Lura, "Internal curing by superabsorbent polymers in ultra-high performance concrete," *Cement and Concrete Research*, vol. 76, pp. 82–90, 2015.

[5] D. Shen, T. Wang, Y. Chen, M. Wang, and G. Jiang, "Effect of internal curing with super absorbent polymers on the relative humidity of early-age concrete," *Construction and Building Materials*, vol. 99, pp. 246–253, 2015.

[6] M. Krafcik, N. Macke, and K. Erk, "Improved concrete materials with hydrogel-based internal curing agents," *Gels*, vol. 3, no. 4, pp. 46–63, 2017.

[7] Y. J. Wang, S. B. Sui, B. Gao, J. L. Xia, H. B. Dong, and Y. X. Li, "Internal curing and its impact on high-strength concrete performance," *The World of Building Materials*, vol. 38, no. 2, pp. 31–34, 2017.

[8] T. Suwan and P. Wattanachai, "Properties and internal curing of concrete containing recycled autoclaved aerated lightweight concrete as aggregate," *Advances in Materials Science and Engineering*, vol. 2017, Article ID 2394641, 11 pages, 2017.

[9] V.-T.-A. Van, C. Rößler, D.-D. Bui, and H.-M. Ludwig, "Rice husk ash as both pozzolanic admixture and internal curing agent in ultra-high performance concrete," *Cement and Concrete Composites*, vol. 53, no. 10, pp. 270–278, 2014.

[10] P. Savva and M. F. Petrou, "Highly absorptive normal weight aggregates for internal curing of concrete," *Construction and Building Materials*, vol. 179, pp. 80–88, 2018.

[11] D. Shen, J. Jiang, Y. Jiao, J. Shen, and G. Jiang, "Early-age tensile creep and cracking potential of concrete internally cured with pre-wetted lightweight aggregate," *Construction and Building Materials*, vol. 135, pp. 420–429, 2017.

[12] D. Shen, J. Jiang, J. Shen, P. Yao, and G. Jiang, "Influence of prewetted lightweight aggregates on the behavior and cracking potential of internally cured concrete at an early age," *Construction and Building Materials*, vol. 99, no. 12, pp. 260–271, 2015.

[13] S. Cheng, Z. Shui, R. Yu, T. Sun, and X. Zhang, "Multiple influences of internal curing and supplementary cementitious materials on the shrinkage and microstructure development of reefs aggregate concrete," *Construction and Building Materials*, vol. 155, pp. 522–530, 2017.

[14] S. Iffat, T. Manzur, and M. A. Noor, "Durability performance of internally cured concrete using locally available low cost LWA," *KSCE Journal of Civil Engineering*, vol. 21, no. 4, pp. 1256–1263, 2016.

[15] M. I. Mousa, M. G. Mahdy, A. H. Abdel-Reheem, and A. Z. Yehia, "Self-curing concrete types; water retention and durability," *Alexandria Engineering Journal*, vol. 54, no. 3, pp. 565–575, 2015.

[16] J. Liu, C. Shi, X. Ma, K. H. Khayat, J. Zhang, and D. Wang, "An overview on the effect of internal curing on shrinkage of high performance cement-based materials," *Construction and Building Materials*, vol. 146, pp. 702–712, 2017.

[17] G. R. de Sensale and A. F. Goncalves, "Effects of Fine LWA and SAP as internal water curing agents," *International Journal of Concrete Structures and Materials*, vol. 8, no. 3, pp. 229–238, 2014.

[18] U. S. Agrawal and S. P. Wanjari, "Physiochemical and engineering characteristics of cenosphere and its application as a lightweight construction material–a review," *Materials Today: Proceedings*, vol. 4, no. 9, pp. 9797–9802, 2017.

[19] A. Hanif, Z. Lu, and Z. Li, "Utilization of fly ash cenosphere as lightweight filler in cement-based composites–a review," *Construction and Building Materials*, vol. 144, pp. 373–384, 2017.

[20] N. Barbare, A. Shukla, and A. Bose, "Uptake and loss of water in a cenosphere-concrete composite material," *Cement and Concrete Research*, vol. 33, no. 10, pp. 1681–1686, 2003.

[21] F. Liu, J. Wang, X. Qian, and J. Hollingsworth, "Internal curing of high performance concrete using cenospheres," *Cement and Concrete Research*, vol. 95, pp. 39–46, 2017.

[22] P. Chen, J. Wang, F. Liu, X. Qian, Y. Xu, and J. Li, "Converting hollow fly ash into admixture carrier for concrete," *Construction and Building Materials*, vol. 159, pp. 431–439, 2018.

[23] D. P. Bentz and K. A. Snyder, "Protected paste volume in concrete," *Cement and Concrete Research*, vol. 29, no. 11, pp. 1863–1867, 1999.

[24] S. Zhutovsky, K. Kovler, and A. Bentur, "Revisiting the protected paste volume concept for internal curing of high-strength concretes," *Cement and Concrete Research*, vol. 41, no. 9, pp. 981–986, 2011.

[25] Y. Wei, Y. Xiang, and Q. Zhang, "Internal curing efficiency of prewetted LWFAs on concrete humidity and autogenous shrinkage development," *Journal of Materials in Civil Engineering*, vol. 26, no. 5, pp. 947–954, 2014.

[26] Y. Xie, S. D. McAllister, D. B. Edwards, and I. F. Cheng, "Fabrication of porous hollow glass microspheres," *Journal of Power Sources*, vol. 196, no. 24, pp. 10727–10730, 2011.

[27] ASTM International, *Standard Test Method for Relative Density (Specific Gravity) and Absorption of Fine Aggregate*, ASTM C128-15, West Conshohocken, PA, USA, 2015.

[28] ASTM International, *Practice for Maintaining Constant Relative Humidity by Means of Aqueous Solutions*, ASTM E104, West Conshohocken, PA, USA, 2012.

[29] O. M. Jensen, "Thermodynamic limitation of self-desiccation," *Cement and Concrete Research*, vol. 25, no. 1, pp. 157–164, 1995.

[30] Y. Wei, W. Guo, and X. Zheng, "Integrated shrinkage, relative humidity, strength development, and cracking potential of internally cured concrete exposed to different drying conditions," *Drying Technology*, vol. 34, no. 7, pp. 741–752, 2015.

[31] J. Zhang, Y. Han, and J. Zhang, "Evaluation of shrinkage induced cracking in concrete with impact of internal curing and water to cement ratio," *Journal of Advanced Concrete Technology*, vol. 14, no. 7, pp. 324–334, 2016.

[32] J. T. Kevern and Q. C. Nowasell, "Internal curing of pervious concrete using lightweight aggregates," *Construction and Building Materials*, vol. 161, pp. 229–235, 2018.

[33] S. Nie, S. Hu, F. Wang et al., "Internal curing–a suitable method for improving the performance of heat-cured concrete," *Construction and Building Materials*, vol. 122, pp. 294–301, 2016.

[34] D. Shen, M. Wang, Y. Chen, T. Wang, and J. Zhang, "Prediction model for relative humidity of early-age internally cured concrete with pre-wetted lightweight aggregates," *Construction and Building Materials*, vol. 144, pp. 717–727, 2017.

[35] K. O. Kjellsen, R. J. Detwiler, and O. E. Gjørv, "Development of microstructures in plain cement pastes hydrated at different temperatures," *Cement and Concrete Research*, vol. 21, no. 1, pp. 179–189, 1991.

[36] Q. J. Li, G. Z. Li, and C. C. Jiang, "Study on the properties of physical and chemical foaming concrete," *Advanced Materials Research*, vol. 549, no. 4, pp. 741–744, 2012.

[37] A. Hajimohammadi, T. Ngo, and P. Mendis, "Enhancing the strength of pre-made foams for foam concrete applications," *Cement and Concrete Composites*, vol. 87, pp. 164–171, 2018.